GEOLOGY

The growth of lithospheric diamonds

Hélène Bureau[1]*, Laurent Remusat[1], Imène Esteve[1], Daniele L. Pinti[2], Pierre Cartigny[3]

Natural diamonds contain mineral and fluid inclusions that record diamond growth conditions. Replicating the growth of inclusion-bearing diamonds in a laboratory is therefore a novel diagnostic tool to constrain the conditions of diamond formation in Earth's lithosphere. By determining the carbon isotopic fractionation during diamond growth in fluids or melts, our laboratory experiments revealed that lithospheric monocrystalline and fibrous and coated diamonds grow similarly from redox reactions at isotopic equilibrium in water and carbonate-rich fluids or melts, and not from native carbon. These new results explain why most of the lithospheric diamonds are characterized by a common carbon isotopic fingerprint, inherited from their common parent fluids and not from the mantle assemblage.

INTRODUCTION

There is now a consensus that diamond growth in Earth's upper mantle is related to carbon precipitation from mobile C-O-H-N-S-Cl fluids/melts, the detailed nature of which remains to be investigated (*1*–*7*). However, the associated carbon speciation (that is, redox state, carbonate melt or fluid, methane, elemental, or carbide) and origin (that is, mantle versus recycled and/or a mixture of both) are still debated (*4*–*6*). In particular, whether monocrystalline (gem-like) diamonds—and the so-called fibrous or coated diamonds—could form from the same parental medium is uncertain. Each of them would have markedly distinct genesis ages; the former are generally described as diamond xenocrysts in their host kimberlite, whereas the latter have short residence times (approximately on a scale of million years) in the mantle and are probably related to kimberlite magmatism (*4*, *5*). Conversely, recent evidence has indicated a shared growth medium (*7*–*9*). Furthermore, fibrous diamonds record a wide variety of fluids that are saline, hydrous, and carbonatitic in nature (*1*, *10*). It remains unclear how these fluids are related. Some studies suggest that immiscibility processes (from a carbonatitic fluid) would govern the chemical diversity (*10*). Others (*11*) suggest that a single original saline fluid would lead to two evolved fluids (carbonatitic and hydrous silicic) depending on the chemical composition of the host rocks. These two opposing models are important to distinguish, as they propose distinct carbon source regions, namely, the asthenosphere and the subduction zones, respectively. C isotopes are central to the discussion and validation of these models, but how carbon behaves during diamond growth remains uncertain. For example, isotopic equilibrium is generally assumed but has never been demonstrated (*5*). In natural systems, diamond generally lacks its original host rock, so addressing these issues is generally not possible. The study of synthetic inclusion-bearing diamonds, while difficult to perform, presents an alternative with which to circumvent this problem.

RESULTS

We produced syngenetic inclusion-bearing diamonds from fluids having different chemical compositions, real proxies for the peridotite-suite lithospheric diamonds and likely for the eclogite suite (*9*). Their carbon isotopic signature was measured at the micrometric scale using secondary ion mass spectrometry (NanoSIMS) (see Materials and Methods). The inclusion-bearing diamonds were grown on synthetic diamond seeds, from fluids under conditions representative of Earth's lithosphere (that is, pressure, temperature, composition, and fO_2). These fluids are identical in chemical composition to the bulk composition of inclusions found in natural fibrous diamonds (*1*) and in some monocrystalline diamonds (*11*). Their composition includes up to 50 weight % water (pure, and saline up to 30 g/liter of NaCl), silicates, carbonates, and graphite (added as a second potential carbon source). Experiments were performed under pressures of 7 to 9 GPa and temperatures from 1200° to 1675°C (see the Supplementary Materials). Homogeneous diamond growth (that is, spontaneous nucleation) and heterogeneous growth (on seeds) were observed. The growth on seeds was significant (maximum oriented overgrowth from 4 to 10 μm in a few hours) and was associated with the trapping of multiphased inclusions: minerals—including spontaneously grown diamonds (that is, diamond included in diamond: "diamond inclusions," up to 3 μm in size at 1400°C; Fig. 1)—and fluids. The silicate assemblage trapped as inclusions in the newly grown diamond is also present in the solid matrix (that is, solid residue associated to the seeds after the experimental quench) associated to the diamonds. For sample H3913 (iron present), this assemblage is comparable to that observed in natural diamonds, such as olivine and Ca,Mg carbonate (that is, dolomite) inclusions (table S1). These results support the hypothesis that mineral and fluid inclusions are syngenetic with their host diamonds (*4*) (that is, formed simultaneously from the same melt or fluid). The syngenicity relationship between inclusions and diamonds is still highly debated today (*12*, *13*), and the present experiments suggest synchronous trapping. Results show that monocrystalline and fibrous diamonds can be grown from the same parent fluids; they differ only in their habit because of varying supersaturation conditions (that is, growth conditions), as previously suggested (*9*, *14*) and in agreement with the study of natural twinned diamond monocrystals having trapped their parent fluids at their interface (*7*). This is also supported by the presence of interfacial hydrous silicic fluid films between mineral inclusions and their host diamonds (*15*), interpreted as relics of the diamond parent fluids.

Diamonds with significant growth on seeds (Fig. 1) were cut with a focused ion beam (FIB) into 2- to 5-μm-thick slices containing inclusions, in order to expose the inclusion areas (Fig. 2). The carbon stable isotope composition of the starting materials was measured by conventional mass spectrometry, and that of the samples and starting seeds was measured by NanoSIMS. Table S1 shows the compositions of the slices as measured by NanoSIMS. The three investigated samples

[1]Institut de Minéralogie, de Physique des Matériaux et de Cosmochimie, Sorbonne Université, UMR CNRS 7590, Muséum National d'Histoire Naturelle, IRD UR 206, 4 Place Jussieu, 75252 Paris Cedex 05, France. [2]GEOTOP and Département des sciences de la Terre et de l'atmosphère, Université du Québec à Montréal, CP 8888, Succ. Centre-Ville, Montréal, Québec H3C 3P8, Canada. [3]LGIS, Institut de Physique du Globe de Paris, Université D. Diderot, UMR CNRS 7154, Paris, France.
*Corresponding author. Email: helene.bureau@impmc.upmc.fr

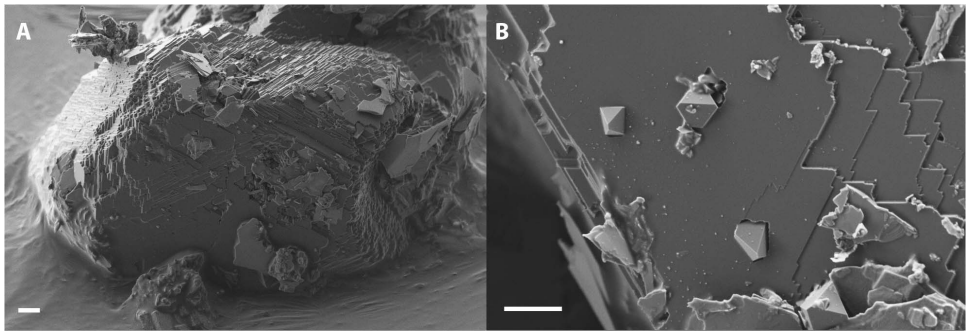

Fig. 1. Secondary electron mapping (SEM) images of a loose diamond extracted from the run products of sample H3908 by mechanical deposition on a stub covered with carbon tape before FIB preparation. (**A**) Diamond growth covers the whole initial seed. (**B**) Close-up of the surface exhibiting the formation and trapping of new spontaneously nucleated diamond crystals as inclusions. Scale bar, 2 μm.

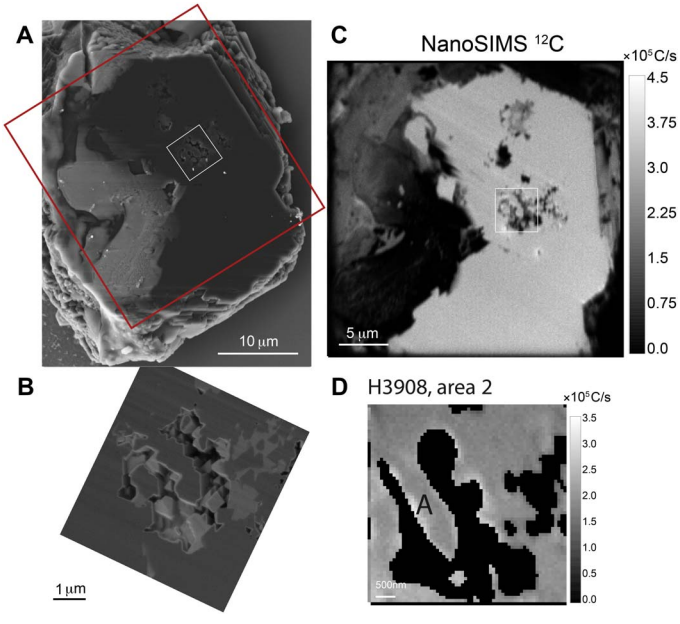

Fig. 2. Sample H3908; upper left corner. (**A**) SEM image of a 5- to 8-μm-thick diamond seed plate containing inclusions resulting from FIB preparation. The plate was extracted with a micromanipulator and deposited on a silicon wafer previously placed in the sample chamber of the FIB. Red box, 30 μm × 30 μm; white box corresponding to inclusions, 25 μm^2 area. (**B**) Close-up of a SE-SEM image of the area showing multiphased inclusions. Gray-level contrasts are density-dependent: dark gray, diamond (including diamond inclusions at the center of the image); medium gray, carbonates; and light gray, SiO_2 (that is, coesite at 7 GPa). (**C**) Large NanoSIMS ^{12}C map of the plate. (**D**) ^{12}C mapping of the 25 μm^2 area including the inclusions. "A" corresponds to diamond inclusions.

HBD01 (7 GPa, 1675°C), H3908 (7 GPa, 1400°C; Fig. 1), and H3913 (7 GPa, 1400°C) are described in detail in table S2. For all the experiments, the potential carbon sources are synthetic graphite and powders containing carbonates [MELD: pure amorphous $CaCO_3$, Na_2CO_3, K_2CO_3; MELD SID: MELD, natural siderite $(Fe,Mg)CO_3$; see table S2].

For clarity, these results are presented in Fig. 3 together with the $\delta^{13}C$ composition of the starting materials. The detailed results are reported as $\delta^{13}C$ in table S1, and the corresponding isotopic maps are also provided in the Supplementary Materials (fig. S3).

DISCUSSION

The $\delta^{13}C$ signature of a diamond depends on the carbon source and its speciation and is redox-sensitive (*5*). In nature, monocrystalline diamonds—including both fibrous and coated diamonds—fall within a narrow range of $\delta^{13}C$ of −5 ± 3‰ (per mil), defining, together with other mantle products, mantle-derived carbon (*5*), not corresponding to either a surface carbonate [from −3 to +4‰ (*5*)] or organic matter [from −45 to −15‰ (*5*)]. Lithospheric diamonds from the eclogitic suite exhibit a significantly larger range, from approximately −40 to 3‰ (*5*). Some diamonds from the transition zone reach −25‰ (*5*), which suggests recycled organic carbon at subduction zones as a potential carbon source for both eclogitic diamonds from the lithosphere and below (*16*). The bulk carbon isotope value for a given diamond may not always reflect those of the components that contributed to its formation. One single diamond can exhibit internal isotopic heterogeneities at the submillimeter scale (*14*, *17*–*19*), attributable to either multistage growth from isotopically distinct or evolving sources (*17*, *18*) or the progressive chemical and/or isotopic evolution of the fluid from which the diamond grew (*14*, *19*).

The $\delta^{13}C$ compositions of some samples fall between the composition of the starting diamond seeds and the composition of the carbonate mixtures, which we attribute to an overlap during analysis. For samples H3913 and H3908 (7 GPa, 1400°C), respectively, the signature of a "new" diamond area ($\delta^{13}C = -17.9 \pm 4.4$‰) and of a diamond inclusion (that is, a diamond spontaneously grown in the fluid and subsequently trapped as an inclusion in diamond; $\delta^{13}C = -14.19 \pm 3.1$‰; see Fig. 2) was determined by quantitative isotope maps. These were compared to the bulk composition (that is, the average isotopic composition of the system) and calculated for all samples following the equation: $\delta^{13}C_{bulk} = x\delta^{13}C_{carbonatepowder} + y\delta^{13}C_{graphite}$, where x and y are the weight fractions of both components loaded in the Pt capsules for each experiment, and where $x + y = 1$.

For sample HBD01, the experiment was performed at high temperature (1645°C). In this run, graphite participated in the diamond growth, resulting in a diamond $\delta^{13}C$ (−24.5 to −27.6‰) very close to that of the graphitic source material (−26.35‰). This result is in agreement with diamond growth experiments performed in the Fe-Ni-C system, with pure graphite as the carbon source (*20*), and is confirmed by the absence of residual graphite in the quenched products associated with the seeds. Although this experiment is not a relevant proxy for Earth's mantle—being far from the geotherm—it illustrates the strong effect of temperature on the nature and behavior of the diamond parent fluid, making graphite available as a carbon source, resulting in a distinct isotopic

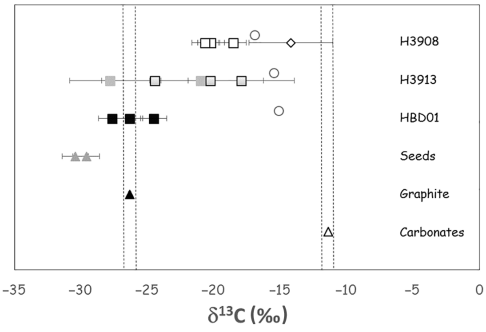

Fig. 3. Carbon isotopic compositions of both starting materials and newly synthesized diamonds. The starting materials are as follows: diamond seeds (gray triangles), graphite (dark triangle), and carbonate powders MELD and MELD + SIDERITE (white triangle); diamond samples are as follows: HBD01 (dark squares), H3913 (gray squares with black rims for the three fragments from map 2), and H3908 (white squares and white diamond are diamond inclusions). The areas delimited by dotted dark lines represent the two potential starting carbon sources: carbonates (MELD and MELD SID) and graphite. The gray triangles represent the composition of the starting diamond seeds. The isotopic composition of the bulk system (all carbon from graphite plus all carbon from carbonates) is calculated for each sample by mass balance and is presented as white circles: Bulk = $x\delta^{13}C_{carbonate} + y\delta^{13}C_{graphite}$, with x and y being initial mass proportions of carbonates and graphite, respectively. For this calculation, no fractionation coefficient is used because this is total mixing. The isotopic compositions of the samples range from the compositions of the starting seeds to those of the carbonate powders, reflecting mixing between the composition of the starting diamond seeds and the newly grown diamond areas. The diamond inclusions from sample H3908 exhibit a $\delta^{13}C$ of −14.2‰, corresponding to a maximum fractionation $\Delta^{13}C$ of −2.74‰ (within error bars) with the carbonate source MELD (carbonates).

composition. The lower-temperature diamond $\delta^{13}C$ compositions (1400°C) cannot originate from the graphite source (−26.3 ± 0.1‰) by a direct dissolution of graphite in the fluid, followed by diamond growth, because the corresponding isotopic fractionation would be limited (*5*). For sample H3908, comparison of the C isotopic bulk signature (−16.9‰) with that of the diamond included in the diamonds (−14.19 ± 3.1‰) shows that the inclusions could not have been generated from a fluid where all the available carbon (graphite and carbonates) would be dissolved [that is, a fluid with the composition of the bulk system (see Fig. 3 and table S3)]. Although we cannot rule out the possibility that a small amount of graphite could have been dissolved in the carbonate fluid or melt during the low-temperature experiments (1400°C), the presence of large graphite globules in the quenched products of samples H3913 and H3908 [up to 400 µm in diameter in 1 mm (diameter) × 1 to 2 mm (length) Pt capsules] implies that graphite is not significantly involved in diamond formation. The presence of dolomite (Ca,Mg carbonate) in the quenched products also demonstrates that carbonates were present in excess during the experiment, confirming that no carbon is needed from graphite to grow diamond. The absence of alkali carbonates in both the quenched matrix and as inclusions also suggests that these carbonates may act as major carbon sources.

The aqueous fluid and carbonate/silicate melt (*8*, *9*) nature of the trapped inclusions also indicates the presence of two fluids in equilibrium with each other at high pressure and high temperature: a hydrous carbonate/silicate melt and an aqueous fluid, both enriched in carbon. If this were the case, the two fluids should be very close to miscibility at the pressure and temperature of the experiment (*8*), which means that they are close in composition and density, with all elements partitioning converging to unity (*21*). Therefore, as they should both exhibit the same $\delta^{13}C$ composition, we deduce that the isotopic composition of the parent fluid is that of the starting carbonated silicate powder (MELD, −11.4 ± 0.1‰).

Diamond growth is proposed to occur through redox reactions with COH fluids from either carbonate or CO_2 reduction (*3*, *14*, *22*) or from CH_4 oxidation (*5*, *23*, *24*) and through oxygen-conserving reactions in a water-rich fluid buffering the system and in which minor coexisting CH_4 or CO_2 reacts to form diamond by precipitation (*25*). Depending on the processes and sources involved during diamond growth, and because the fractionation between ^{12}C and ^{13}C is dependent on phase transformation processes and on carbon speciation in fluids, the carbon isotopes would be fractionated to different degrees. Core-to-rim variations of the $\delta^{13}C$ in diamonds are known indicators of redox processes: At 1000°C and under isotopic equilibrium, diamond is enriched in ^{13}C by approximately 2 to 3‰ compared to carbonate or CO_2 but is depleted in ^{13}C by approximately 1‰ when it precipitates from CH_4 (*5*). A reoxidation of Fe-Ni-C phases would involve a fractionation factor from 4.1 to 2.4‰ at 1450°C (*20*), whereas a precipitation process from dissolved carbon (no redox reaction) would cause a depletion of only a few tenths of a per mil (*5*). The diamond inclusions present in seeds from sample H3908 (Fig. 2) represent new uncontaminated diamond crystals. Therefore, we can use their isotopic composition to calculate the $\Delta_{carbonatefluid\text{-}diamond} = \delta^{13}C_{carbonatefluid} - \delta^{13}C_{diamond} \approx 10^3 \ln\alpha_{carbonate\text{-}diamond}$ (where $\alpha_{carbonatefluid\text{-}diamond}$ is the factor of $^{12}C/^{13}C$ fractionation). We obtain a $\Delta_{carbonatefluid\text{-}diamond}$ of 2.8‰, in agreement with diamond formation from fluid or melt: A calculation performed assuming isotopic equilibrium at 1400°C predicts that diamond should be depleted in ^{13}C by 2 to 4‰ compared to its carbonate or CO_2 source (*5*). This is also in agreement with diamond synthesis from pure sodium oxalate acting as the carbon source: $\Delta_{carbonatefluid\text{-}diamond}$ = 2.6‰ at 7.5 GPa and 1400° to 1700°C (*26*). The low-temperature samples of the present study are relevant proxies for natural lithospheric diamonds, and their isotopic signatures show that all lithospheric diamonds, whether monocrystalline or fibrous, grow from oxidized carbon species dissolved in hydrous melt or fluids through redox mechanisms involving carbonate fluid or melt reduction (oxidized). For the present experiments, we propose the following two reactions (Equations 1 and 2):

$$12Al_2O_3 + 4MgO + K_2CO_3 + 16SiO_2 + 4H_2O + 2CO_2 = 4K(Al, Mg)_2(OH)_2(Si, Al)_4O_{10phengite} + 4C_{Diamond} + 19O_2 \quad (1)$$

$$Al_2O_3 + 3MgO + 2(Fe, Mg)CO_3 + 3SiO_2 + 2K_2CO_3 + 2Na_2CO_3 + 3CaCO_3 + 2H_2O + 2CO_2 = (Fe, Mg)_2SiO_{4olivine} + MgAl_2O_{4spinel} + 10C_{Diamond} + 12O_2 + (Ca, Mg)CO_3 + 2(Na, K)_2(Ca, Mg)Al_2SiO_7H_2O_{Glass} \quad (2)$$

with H_2O and carbonates (possibly some aqueous CO_2 and/or carbonate groups CO_3^{2-}) being present in either the hydrous carbonatitic melt or the aqueous fluid (in chemical and isotopic equilibrium with each other).

Experiments performed under upper mantle conditions show that carbon isotopic fractionation is controlled by temperature, bulk composition, and the redox conditions (*27*). For experiment H3913 (iron present), olivine and diamond are produced; for this experiment, the starting materials were synthetic powders. We cannot calculate the

oxygen fugacity, but on the basis of the presence of olivine and dolomite, we can assume that fO_2 is close to FMQ-1 or FMQ-2 (fayalite + O_2 = magnetite + quartz), similar to EMOD (enstatite + magnesite = olivine + diamond). In experiments performed under comparable conditions (diamond seeds, silicate and carbonate powders, and water), but without graphite in the starting materials, no diamond growth is observed [that is, exp. #211 (*9*)], in agreement with previous results (*28*), likely reflecting fO_2 conditions above EMOD. Therefore, the presence of graphite determines growth versus dissolution during the experiments, by buffering the redox of the system, acting as a fO_2 buffer and not as a C source. In the same fluid or melt, under less-reducing conditions (that is, with no graphite buffer present), diamond does not grow or is dissolved (*9*, *28*). Under more-reducing conditions (that is, with a graphite buffer present), diamond grows (*8*, *9*, *22*). This dependence on oxygen fugacity constrains the location of diamond formation in the mantle. Because the same primitive fluids and their immiscible products will lead to fibrous and monocrystalline diamond growth, they account for their common carbon isotopic composition.

A significant amount of carbon must be present in the upper mantle (*29*), possibly as fluids or melts located at the lithosphere-asthenosphere boundary (*30*, *31*), before they are converted to diamonds when redox becomes favorable to growth.

MATERIALS AND METHODS

Sample preparation

FIB preparation was performed on a selection of diamonds: HBD01, H3908, and H3913 (fig. S1 and table S1). The diamonds were deposited on stubs covered with carbon tape. The selected diamonds were sliced open on one face and polished by the ion beam. Those that exhibited inclusions were sliced and ion beam–polished on the other face in order to obtain 2- to 5-μm-thick sections, including the trapped inclusions. The thick diamond sections were extracted and deposited with a FIB micromanipulator on silicon wafers and gold-coated for NanoSIMS measurements (fig. S2). The starting diamond seeds were embedded in indium and polished with the ion beam.

Analytical conditions and calibration for carbon isotope measurement with the NanoSIMS

Samples were coated with 10 nm of gold. The size (<10 μm) of the growth areas required a nanoscale analysis, which was only possible using the 150-nm NanoSIMS beam. Images were acquired using the NanoSIMS 50 (CAMECA) located at the Museum National d'Histoire Naturelle in Paris, France. Sample surface was sputtered by a 1.5-pA Cs beam to obtain images of various sizes from 5 μm × 5 μm to 30 μm × 30 μm and divided into 256 pixels × 256 pixels. Raster speed was regulated at 1 ms per pixel, with an approximate spatial resolution of 150 nm. Secondary images of ^{12}C, ^{13}C, ^{16}O, and ^{28}Si were simultaneously collected. Before each acquisition, the sample surface was presputtered over a 30 μm × 30 μm region using a 100-pA Cs^+ beam for 10 min to remove gold coating and surface contamination and to reach sputtering steady state. The images were processed using the L'IMAGE software (L. Nittler, Carnegie Institution). ^{13}C and ^{12}C were used to generate $\delta^{13}C$ isotopic compositions, relative to the PDB (Pee Dee Belemnite) standard. Regions of interest were manually drawn to isolate new diamond growth areas and to determine their isotopic composition. The calibration was performed against broken pieces of natural Ia and a synthetic IIa diamond used for diamond anvil cells, whose compositions were determined by gas source mass spectrometry at IPGP (Institut de Physique du Globe de Paris) at −3.6 ± 0.1‰ and −20.9 ± 0.1‰. These carbon isotope compositions were determined by combustion of each diamond, followed by analysis of the resulting CO_2 gas using a Thermo Fisher Delta + XP dual-inlet gas source mass spectrometer. Diamonds were individually wrapped in Pt foil and combusted under vacuum at 1100°C in pure oxygen. Extracted CO_2 gas was purified and gas pressure–quantified for yield evaluation under cryogenic conditions before collection and analysis. The carbon isotopic values obtained for the diamonds are reported as $\delta^{13}C = [(^{13}C/^{12}C)_{sample}/(^{13}C/^{12}C)_{V\text{-}PDB} - 1)] \times 1000$, with an uncertainty of <0.06‰ (2σ). The calibration methodology is presented in the study of Pinti *et al.* (*32*).

The starting materials (powders) used for the experiments were similarly characterized for their $\delta^{13}C$ using gas source mass spectrometry at GEOTOP, Montréal, using three reference standards at −42.16, −28.75, and −11.85‰, respectively, versus VPDB (Vienna Pee Dee Belemnite) with an uncertainty of 0.1‰.

SUPPLEMENTARY MATERIALS

Supplementary material for this article is available at http://advances.sciencemag.org/cgi/content/full/4/6/eaat1602/DC1

table S1. Isotopic compositions of the starting materials, standards, and samples.
table S2. Description of the studied samples.
table S3. Mass balance calculations of isotopic compositions of the bulk composition for the starting materials and the high-pressure and high-temperature carbonate fluid.
fig. S1. SEM images of the FIB preparation, cut on one side of the seed and on the other side to obtain the final slices.
fig. S2. Details of the samples analyzed with the NanoSIMS.
fig. S3. NanoSIMS maps of ^{12}C for each investigated sample showing the locations of the areas of interest (red squares) corresponding to the location of the measurements reported in table S1 and Fig. 1.
Reference (*33*)

REFERENCES AND NOTES

1. O. Navon, I. D. Hutcheon, G. R. Rossman, G. J. Wasserburg, Mantle-derived fluids in diamond micro-inclusions. *Nature* **335**, 784–789 (1988).
2. E. S. Izraeli, J. W. Harris, O. Navon, Brine inclusions in diamonds: A new upper mantle fluid. *Earth Planet. Sci. Lett.* **187**, 323–332 (2001).
3. T. Stachel, J. W. Harris, Formation of diamond in the Earth's mantle. *J. Phys. Condens. Matter* **21**, 364206 (2009).
4. S. B. Shirey, P. Cartigny, D. J. Frost, S. Keshav, F. Nestola, P. Nimis, G. Pearson, N. V. Sobolev, M. J. Walter, Diamonds and the geology of mantle carbon. *Rev. Mineral. Geochem.* **75**, 355–421 (2013).
5. P. Cartigny, M. Palot, E. Thomassot, J. W. Harris, Diamond formation: A stable isotope perspective. *Annu. Rev. Earth Planet. Sci.* **42**, 699–732 (2014).
6. T. Stachel, R. W. Luth, Diamond formation—Where, when and how? *Lithos* **220–223**, 200–220 (2015).
7. B. M. Jablon, O. Navon, Most diamonds were created equal. *Earth Planet. Sci. Lett.* **443**, 41–47 (2016).
8. H. Bureau, F. Langenhorst, A.-L. Auzende, D. J. Frost, I. Estève, J. Siebert, The growth of fibrous, cloudy and polycrystalline diamonds. *Geochim. Cosmochim. Acta* **77**, 202–214 (2012).
9. H. Bureau, D. J. Frost, N. Bolfan-Casanova, C. Leroy, I. Esteve, P. Cordier, Diamond growth in mantle fluids. *Lithos* **265**, 4–15 (2016).
10. O. Klein-BenDavid, D. G. Pearson, G. M. Nowell, C. Ottley, J. C. R. McNeill, P. Cartigny, Mixed fluid sources involved in diamond growth constrained by Sr–Nd–Pb–C–N isotopes and trace elements. *Earth Planet. Sci. Lett.* **289**, 123–133 (2010).
11. Y. Weiss, J. McNeill, D. G. Pearson, G. M. Nowell, C. J. Ottley, Highly saline fluids from a subducting slab as the source for fluid-rich diamonds. *Nature* **524**, 339–342 (2015).
12. E. Thomassot, P. Cartigny, J. W. Harris, J. P. Lorand, C. Rollion-Bard, M. Chaussidon, Metasomatic diamond growth: A multi-isotope study (^{13}C, ^{15}N, ^{33}S, ^{34}S) of sulphide inclusions and their host diamonds from Jwaneng (Botswana). *Earth Planet. Sci. Lett.* **282**, 79–90 (2009).
13. F. Nestola, H. Jung, L. A. Taylor, Mineral inclusions in diamonds may be synchronous but not syngenetic. *Nat. Commun.* **8**, 14168 (2017).
14. S. R. Boyd, F. Pineau, M. Javoy, Modelling the growth of natural diamonds. *Chem. Geol.* **116**, 29–42 (1994).

15. P. Nimis, M. Alvaro, F. Nestola, R. J. Angel, K. Marquardt, G. Rustioni, J. W. Harris, F. Marone, First evidence of hydrous silicic fluid films around solid inclusions in gem-quality diamonds. *Lithos* **260**, 384–389 (2016).
16. R. Tappert, T. Stachel, J. W. Harris, K. Muehlenbachs, T. Ludwig, G. P. Brey, Subducting oceanic crust: The source of deep diamonds. *Geology* **33**, 565–568 (2005).
17. S. Mikhail, A. B. Verchovsky, D. Howell, M. T. Hutchison, R. Southworth, A. R. Thomson, P. Warburton, A. P. Jones, H. J. Milledge, Constraining the internal variability of the stable isotopes of carbon and nitrogen within mantle diamonds. *Chem. Geol.* **366**, 14–23 (2014).
18. G. P. Bulanova, D. F. Wiggers de Vries, D. G. Pearson, A. Beard, S. Mikhail, A. P. Smelov, G. R. Davies, An eclogitic diamond from Mir pipe (Yakutia), recording two growth events from different isotopic sources. *Chem. Geol.* **381**, 40–54 (2014).
19. P. Cartigny, J. W. Harris, A. Taylor, R. Davies, M. Javoy, On the possibility of a kinetic fractionation of nitrogen stable isotopes during natural diamond growth. *Geochim. Cosmochim. Acta* **67**, 1571–1576 (2003).
20. V. N. Reutsky, Y. M. Borzdov, Y. N. Palyanov, Effect of diamond growth rate on carbon isotope fractionation in Fe–Ni–C system. *Diam. Relat. Mater.* **21**, 7–10 (2012).
21. H. Bureau, E. Foy, C. Raepsaet, A. Somogyi, P. Munsch, G. Simon, S. Kubsky, Bromine cycle in subduction zones through in situ Br monitoring in diamond anvil cells. *Geochim. Cosmochim. Acta* **74**, 3839–3850 (2010).
22. Y. N. Palyanov, Y. V. Bataleva, A. G. Sokol, Y. M. Borzdov, I. N. Kupriyanov, V. N. Reutsky, N. V. Sobolev, Mantle–slab interaction and redox mechanism of diamond formation. *Proc. Natl. Acad. Sci. U.S.A.* **110**, 20408–20413 (2013).
23. E. Thomassot, P. Cartigny, J. W. Harris, K. S. Viljoen, Methane-related diamond crystallization in the Earth's mantle: Stable isotope evidences from a single diamond-bearing xenolith. *Earth Planet. Sci. Lett.* **257**, 362–371 (2007).
24. P. Deines, The carbon isotopic composition of diamonds: Relationship to diamond shape, color, occurrence and vapor composition. *Geochim. Cosmochim. Acta* **44**, 943–961 (1980).
25. T. Stachel, T. Chacko, R. W. Luth, Carbon isotope fractionation during diamond growth in depleted peridotite: Counterintuitive insights from modelling water-maximum CHO fluids as multi-component systems. *Earth Planet. Sci. Lett.* **473**, 44–51 (2017).
26. V. Reutsky, Y. Borzdov, Y. Palyanov, A. Sokol, O. Izokh, Carbon isotope fractionation during experimental crystallisation of diamond from carbonate fluid at mantle conditions. *Contrib. Mineral. Petrol.* **170**, 41 (2015).
27. D. J. Frost, C. A. McCammon, The redox state of Earth's mantle. *Annu. Rev. Earth Planet. Sci.* **36**, 389–420 (2008).
28. A. F. Khokhryakov, Y. N. Pal'yanov, The evolution of diamond morphology in the process of dissolution: Experimental data. *Am. Mineral.* **92**, 909–917 (2007).
29. R. Dasgupta, Ingassing, storage, and outgassing of terrestrial carbon through geologic time. *Rev. Mineral. Geochem.* **75**, 183–229 (2013).
30. C. Crépisson, G. Morard, H. Bureau, G. Prouteau, Y. Morizet, S. Petitgirard, C. Sanloup, Magmas trapped at the continental lithosphere–asthenosphere boundary. *Earth Planet. Sci. Lett.* **393**, 105–112 (2014).
31. S. Tharimena, C. Rychert, N. Harmon, A unified continental thickness from seismology and diamonds suggests a melt-defined plate. *Science* **357**, 580–583 (2017).
32. D. L. Pinti, A. Ishida, N. Takahata, Y. Sano, H. Bureau, P. Cartigny, Micron-scale $\delta^{13}C$ determination by NanoSIMS in a Juina diamond with a carbonate inclusion. *Geochem. J.* **50**, e7–e12 (2016).
33. G. Slodzian, F. Hillion, F. J. Stadermann, E. Zinner, QSA influences on isotopic ratio measurements. *Appl. Surf. Sci.* **231–232** 874–877 (2004).

Acknowledgments: We thank D. J. Frost and the staff of the Bayerisches Geoinstitut Bayreuth for their constant support during sample synthesis, the NanoSIMS staff at the Muséum d'Histoire Naturelle (MNHN), A. Vitale-Brovarone for fruitful discussions, and S. Palmer for improving the English of the paper. The authors are grateful to the two anonymous reviewers who have provided very constructive comments and to W. Panero. J.-F. Hélie at GEOTOP is thanked for $\delta^{13}C$ measurements on the starting materials. **Funding:** The FIB and SEM facility of IMPMC was supported by Région Ile de France Grant SESAME 2006 NOI-07-593/R, Institut National des Sciences de l'Univers (INSU)–CNRS, Institut de physique–CNRS, Sorbonne Université, and the French National Research Agency (ANR) grant ANR-07-BLAN-0124-01. The National NanoSIMS facility at the MNHN was established by funds from the INSU-CNRS, Region Ile de France, Ministère Délégué à l'Enseignement Supérieur et à la Recherche, and MNHN. The present study was supported by Campus France through the PROCOPE Project 26673WC (H.B.), the DFG grant 54366326 (D.J. Frost), and the Programme de Planétologie of CNRS-INSU cofunded by Centre national d'études spatiales. **Author contributions:** H.B. designed the study, performed the experiments, and wrote the manuscript before all authors commented on it. L.R. and H.B. performed the NanoSIMS analysis; I.E. performed the FIB preparation; P.C., H.B., and D.L.P. contributed to the calibration of NanoSIMS. **Competing interests:** The authors declare that they have no competing interests. **Data and materials availability:** All data needed to evaluate the conclusions in the paper are present in the paper and/or the Supplementary Materials. Additional information may be requested from H.B.

Submitted 30 January 2018
Accepted 25 April 2018
Published 6 June 2018
10.1126/sciadv.aat1602

Citation: H. Bureau, L. Remusat, I. Esteve, D. L. Pinti, P. Cartigny, The growth of lithospheric diamonds. *Sci. Adv.* **4**, eaat1602 (2018).

Science Advances

The growth of lithospheric diamonds

Hélène Bureau, Laurent Remusat, Imène Esteve, Daniele L. Pinti and Pierre Cartigny

Sci Adv **4** (6), eaat1602.
DOI: 10.1126/sciadv.aat1602